Operational characteristics of a 50 W DMFC stack

Daejin Kim, Jaeyoung Lee, Tae-Hoon Lim, In-Hwan Oh, Heung Yong Ha *

Fuel Cell Research Center, Korea Institute of Science and Technology (KIST), P.O. Box 131, Cheongryang, Seoul 130-650, South Korea

Abstract

The characteristics of a 50 W direct methanol fuel cell (DMFC) stack were investigated under various operating conditions in order to understand the behavior of the stack. The operating variables included the methanol concentration, the flow rate and the flow direction of the reactants (methanol and air) in the stack. The temperature of the stack was autonomously increased in proportion to the magnitude of the electric load, but it decreased with an increase in the flow rates of the reactants. Although the operation of the stack was initiated at room temperature, under a certain condition the internal temperature of the stack was higher than 80 °C. A uniform distribution of the reactants to all the cells was a key factor in determining the performance of the stack. With the supply of 2 M methanol, a maximum power of the stack was found to be 54 W (85 mW cm^{-2}) in air and 98 W (154 mW cm^{-2}) in oxygen. Further, the system with counter-flow reactants produced a power output that was 20% higher than that of co-flow system. A post-load behavior of the stack was also studied by varying the electric load at various operating conditions.
© 2005 Elsevier B.V. All rights reserved.

1. Introduction

Because the direct methanol fuel cell (DMFC) consumes methanol and air (or oxygen) as reactants, it has many advantages over other types of fuel cells as a portable power source [1–7]. To generate a sufficient power for portable devices, an appropriately sized DMFC stack consisting of a certain number of unit cells should be fabricated, and the operating conditions should be optimized to enhance the power density of the DMFC system.

DMFC stacks are classified into two types, based on the configuration of electrodes, membrane, and separators. The first type is a monopolar stack, which is assembled by placing electrodes of the same polarity on the same plane of the membrane and then electrically connecting the anodes and cathodes in series [7,8]. Despite the easy supply of reactants, the monopolar stack has a high internal resistance because the electric current should flow along the plane of the electrode strips [9]. The second type of stack is a bipolar design, which

consists of a number of repeated units of a membrane electrode assembly (MEA) and a bipolar plate [10]. The bipolar plate separates each MEA and provides a series of electrical connections between the adjacent cells in the stack. It also supplies reactants to each cell through flow channels formed on both side of the plates. The bipolar stack has lower internal resistance and thus, is adequate for larger stacks than the monopolar design [11].

There have been several reports on DMFC stacks. Dohle et al. [12] developed a DMFC stack consisting of 71 cells with an electrode area of 144 cm^2. The stack with 71 cells showed a power output of 500 W and a power density of 50 mW cm^{-2}. Jiang et al. [11] designed a DMFC stack with a metal foam flow field; it had an average power output of 26 mW cm^{-2}. Buttin et al. [13] demonstrated a 150 W DMFC stack with five cells; by feeding 1 M of methanol and air at 3 atm, the stack had an average power density of about 140 mW cm^{-2} at 110 °C. The main limiting factors in this DMFC stack were attributed to the distribution of reactants and internal resistance. Gogel et al. [14] showed that a DMFC stack made up of 12 cells using Nafion 105 could be operated in a temperature range of 70 °C

* Corresponding author. Tel.: +82 2 958 5275; fax: +82 2 958 5199.
E-mail address: hyha@kist.re.kr (H.Y. Ha).

and 90 °C and exhibited power density about 60 mW cm^{-2} at 0.5 V.

In spite of these reports on the DMFC stacks, more details must be clarified in order to fully understand and to optimize DMFC stacks for their use in portable applications. In this study, we developed a bipolar DMFC stack with six unit cells and investigated the characteristics of the stack under various operating conditions. A comparison was made between single cell and the DMFC stack in terms of performance and temperature change.

2. Experimental

The electro-catalysts used in the anode and the cathode were Pt-Ru black (50:50 at%) and Pt black (Johnson Matthey), respectively, and their loadings in each electrode were 5 mg cm^{-2} based on the total metal weight. A carbon cloth (E-Tek) was used as a substrate for the electrodes and Nafion 115 (DuPont®) was used as an electrolyte membrane. The MEA with an active area of 106 cm^2 was fabricated by hot pressing at 8.0 MPa at 130 °C for 150 s. Graphite bipolar plates of 3 mm thickness were carved mechanically with a serpentine flow field on both sides of the plates.

The stack was composed of six cells connected in series, and it was assembled using homemade housing that comprised aluminum end plates and gold-coated copper plates as current collectors. Fig. 1(a and b) shows a picture and a schematic diagram of the stack, respectively. In the counter-flow system, as shown in Fig. 1(c), a fresh methanol solution was supplied to the anode compartment of the DMFC from
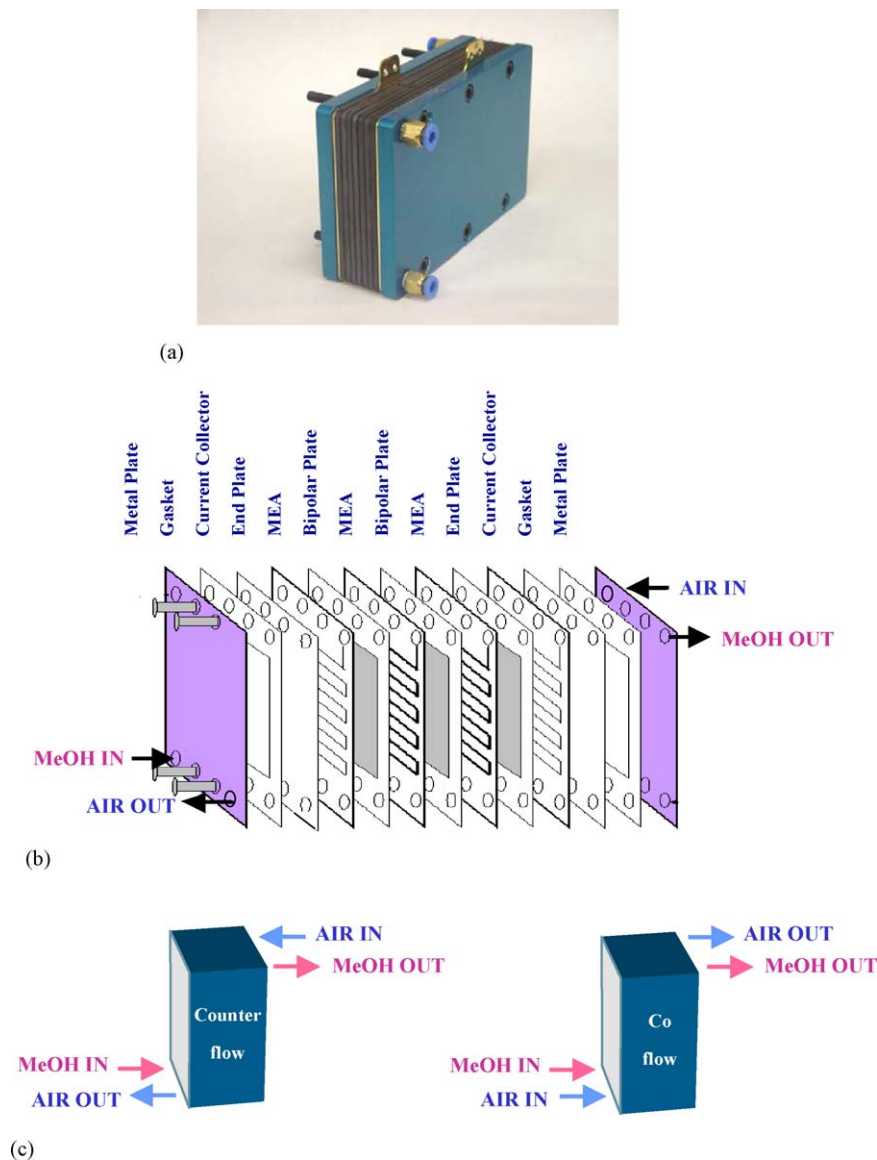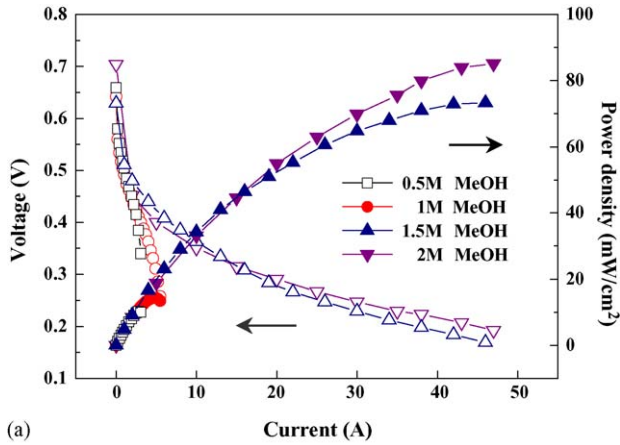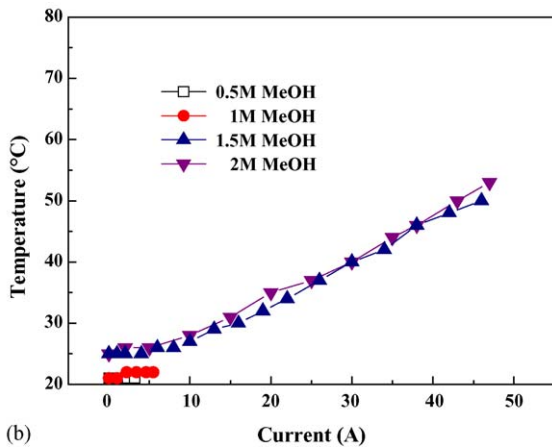

Fig. 1. (a) Photograph of a 50 W class DMFC stack; (b) schematic of a DMFC stack; (c) flow direction of a counter-flow and co-flow on a stack.

site top inlet to help remove the produced water from the cathode.

In the co-flow system, as shown in Fig. 1(d), the methanol solution and the air were fed into the bottom inlets and discharged from the opposite top outlets. The operation of the single cell and the stack began at room temperature without an external heating source, and the temperature of the individual cells in the stack was measured through thermocouples which were put into the holes of the graphite plates close to the MEA. The cell performance was measured using an electronic loader by recording the cell voltage after it had reached a steady value.

3. Results and discussion

Before studying the characteristics of a DMFC stack, we investigated the performance of a single cell with an active area of 106 cm^2 under various operating conditions to obtain reference data for a better understanding of stack operation. Fig. 2(a) shows how methanol concentration affects the performance of DMFCs at given flow rates for the methanol solution (11.25 ml min^{-1}) and air (750 sccm) at room tem-

Fig. 2. (a) Single cell performance and (b) temperature at different methanol concentrations (■: 0.5 M, ●: 1 M, ▲: 1.5 M, ▼: 2 M methanol solution, 750 sccm dry air).

the bottom inlet and discharged from the top outlet with the aid of a peristaltic pump. The unreacted methanol containing CO_2 gas was not reused. Dry air supplied from a cylinder was fed into the cathode compartment at the oppo-
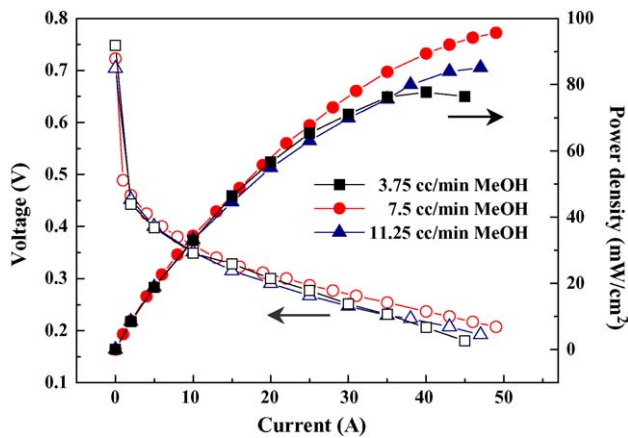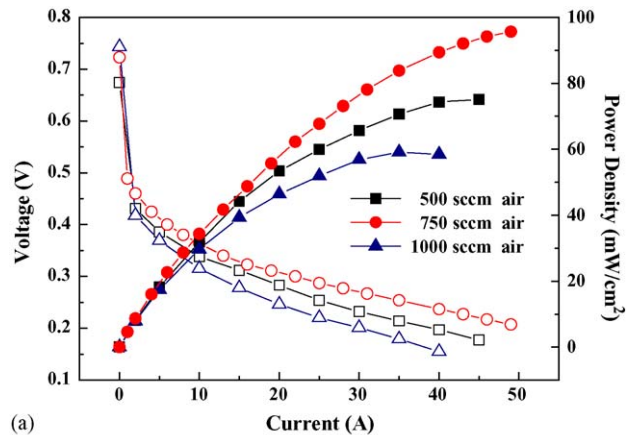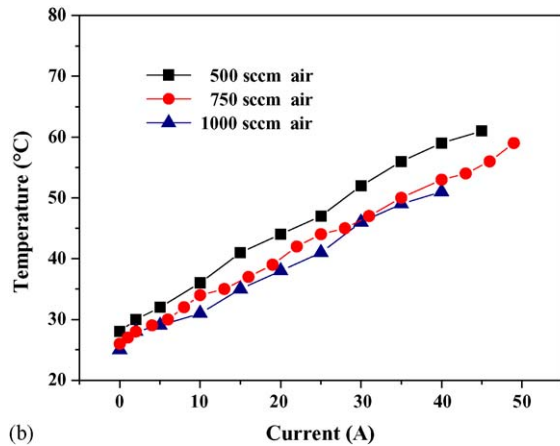

Fig. 3. Single cell performance at different flow rates of 2 M methanol solution (■: 3.75 cm^3 min^{-1}, ●: 7.5 cm^3 min^{-1}, ▲: 11.25 cm^3 min^{-1}, 750 sccm dry air).

Fig. 4. (a) Single cell performance and (b) temperature at different air flow rates (■: 500 sccm, ●: 750 sccm, ▲: 1000 sccm dry air, 7.5 cm^3 min^{-1} 2 M methanol).

perature. The power density of DMFCs increased as the methanol concentration increased. The highest performance of the DMFCs was obtained when a 2 M methanol solution was supplied. However, at lower methanol concentrations, a steep drop in voltage was observed at a current range

higher than 5 A, probably due to the deficiency in the supply of methanol to the anode under the given flow rate of the methanol solution. A higher flow rate is favorable to obtain significant performance with a diluted methanol solution as the feed. According to Ravikumar and Shukla [15],
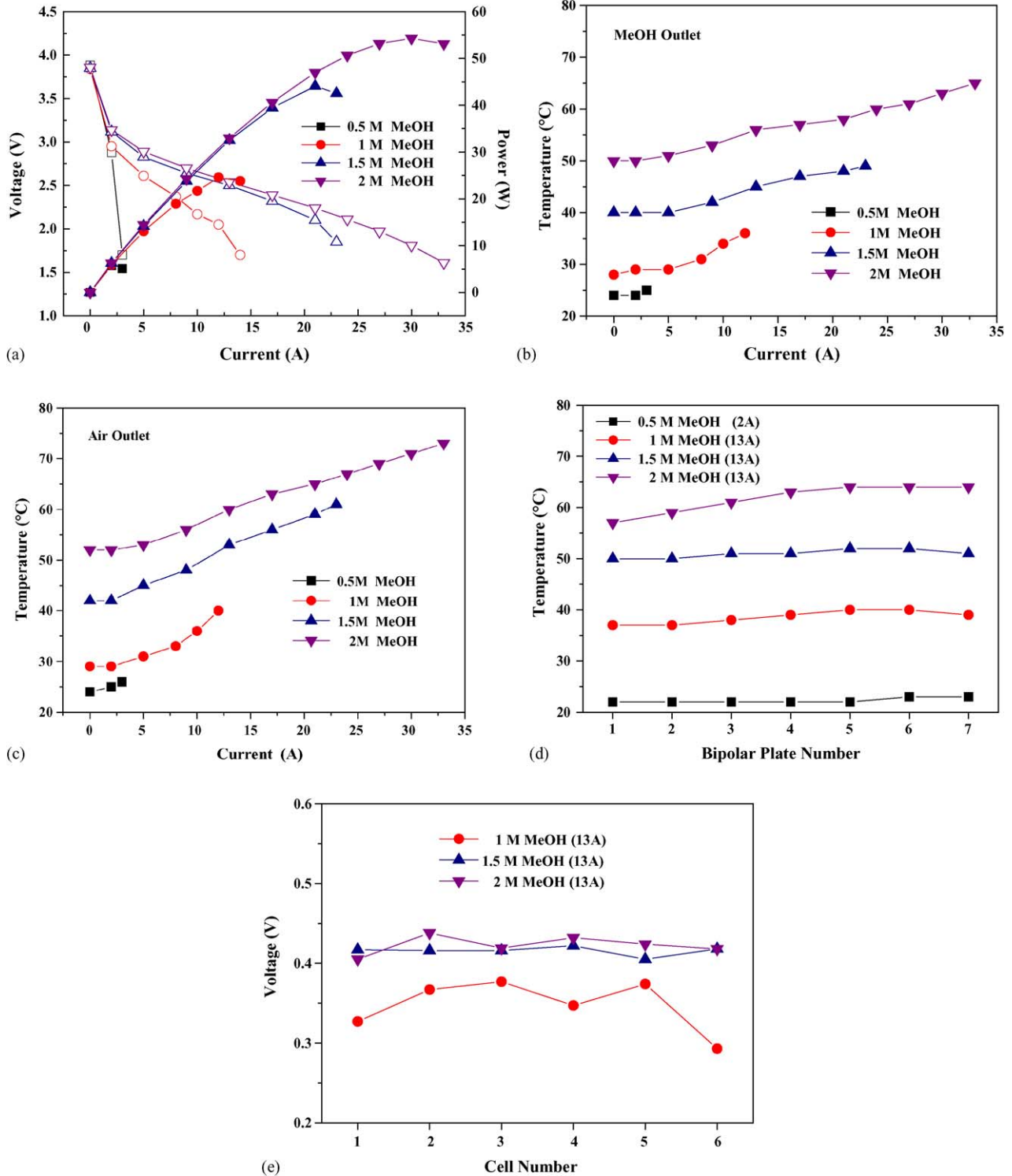

Fig. 5. (a) Stack power, (b) methanol outlet temperature, (c) air outlet temperature, (d) individual bipolar plate temperature, and (e) individual cell voltage at different methanol concentrations (■: 0.5 M, ●: 1M, ▲: 1.5 M, ▼: 2 M methanol solution, 12 slm dry air).

the cell could deteriorate rapidly when exposed to a concentrated methanol solution higher than 2.5 M and thus we limited the methanol concentration to 2.0 M. Fig. 2(b) shows the temperature change of the cell with different methanol concentrations. With methanol concentrations more than 1.5 M the cell temperature autonomously increased as the electric load was increased. The cell temperature eventually reached 53 °C due to the exothermal oxidation of the permeated methanol and the oxygen reduction at the cathode.

Fig. 3 shows the power density at different flow rates of 2 M methanol feed. The power density, which was affected by the flow rate of the methanol solution, reached a maximum value of 95 mW cm^{-2} at 0.21 V and 62 mW cm^{-2} at 0.30 V at 7.5 ml min^{-1}. The cell temperature rose when the electric load increased and the flow rate decreased. The optimum methanol flow rate is the result of a trade-off between facilitating the supply of methanol to the anode, removing the CO$_2$ from the anode, decreasing the cell temperature, and increasing the methanol crossover rate when the methanol flow rate increases.

The air flow rate also influenced the DMFC performance. In Fig. 4(a), we observed a maximum performance at an air flow rate of 750 sccm. In addition, the optimum air flow rate seems to be related to the cell temperature, which is subject to change due to heat dissipation by air. As shown in Fig. 4(b), the cell temperature increases as the electric load increases and the air flow rate decreases. In general, a higher air flow rate is preferred because it facilitates the mass transport of oxygen and the removal of water in the cathode. However, when the DMFC has no external heating source, the cell temperature is readily affected by the air flow rate. Thus, an appropriate air flow rate should be chosen to maximize the oxygen transport while minimizing the temperature drop in the cell.

On the basis of experimental observation of the single cells, we designed a stack consisting of six unit cells, as shown in Fig. 1. The stack specifications are given in Table 1. At first, the stack was operated in a counter-flow scheme as shown in Fig. 1(c), and its performance was measured under various operating conditions at room temperature without back pressure. Cell 1 was sandwiched between bipolar
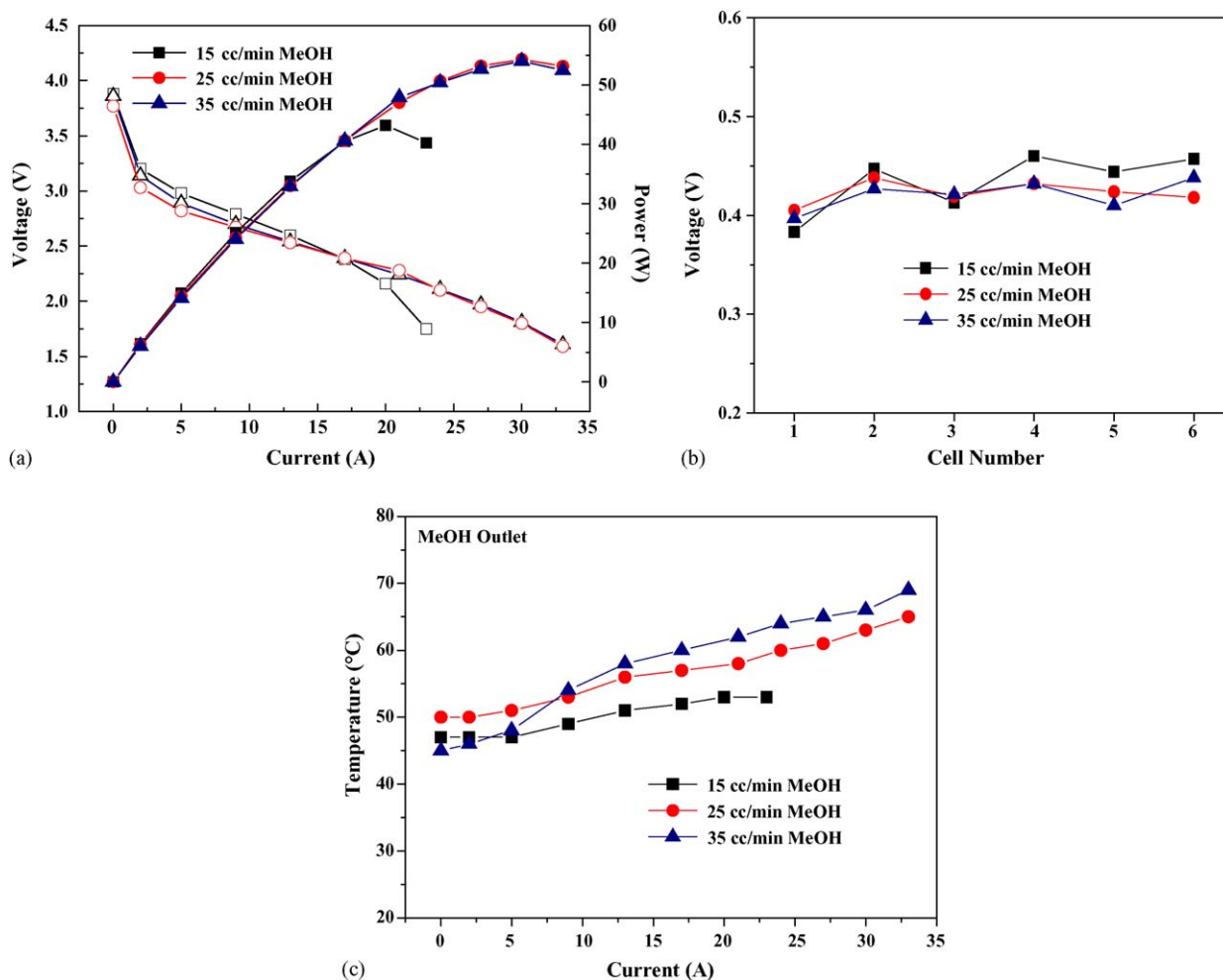

Fig. 6. (a) Stack power, (b) individual cell voltage, and (c) methanol outlet temperature at different flow rates of 2 M methanol (■: 15 cm^3 min^{-1}, ●: 25 cm^3 min^{-1}, ▲: 35 cm^3 min^{-1}, 2 M methanol, 12 slm dry air).

Table 1
Specification of a 50 W class DMFC stack

MEA	Membrane	Nafion 115
	Anode	Pt-Ru black 5 mg cm^{-2}
	Cathode	Pt black 5 mg cm^{-2}
STACK	Number of cells	6
	Electrode area	106 cm^2
	Cell pitch	3.8 mm
	Size	49 mm × 105 mm × 161 mm
	Temperature	Room temperature
	Reactants	25 cm^3 min^{-1} 2 M methanol, 12 slm air
Maximum performance	Total	54 W, 90 mW cm^{-2}

plates (BP) 1 and 2, while cell 6 was between BP 6 and BP 7.

Fig. 5 shows the way in which the methanol concentration affects the performance of the stack, and it has been found that 2 M methanol feeding resulted in a maximum stack performance of 54 W at 1.8 V. Fig. 5(b) shows the temperatures at the methanol outlets, while Fig. 5(c) shows the temperatures at the air outlets. In these figures, one can see that even in the open circuit the temperature is higher than the room temperature of 25 °C; moreover, it is almost proportional to the methanol concentration and reached 50 °C with a 2 M methanol feed. This result shows the considerable contribution of the methanol crossover during the temperature rise.

The temperature increased further when we applied an electric load. Due to the exothermic reduction of oxygen, the electric load generated heat at the cathode and the temperature reached 65 °C at 33 A with a 2 M methanol feed (see Fig. 5(b)). The temperature of the air stream at the outlet shown in Fig. 5(c) shows almost the same pattern as that of temperature at the methanol outlet. However, the air temperature was higher than the methanol temperature, and the difference became larger as the electric load increased. In Fig. 5(d), the individual cell temperatures, which were measured at each bipolar plate at a current of 13 A, increased and became uniform as the methanol concentration increased. Fig. 5(e) shows the voltage distribution over the individual cells of the stack at a current of 13 A. Below a methanol
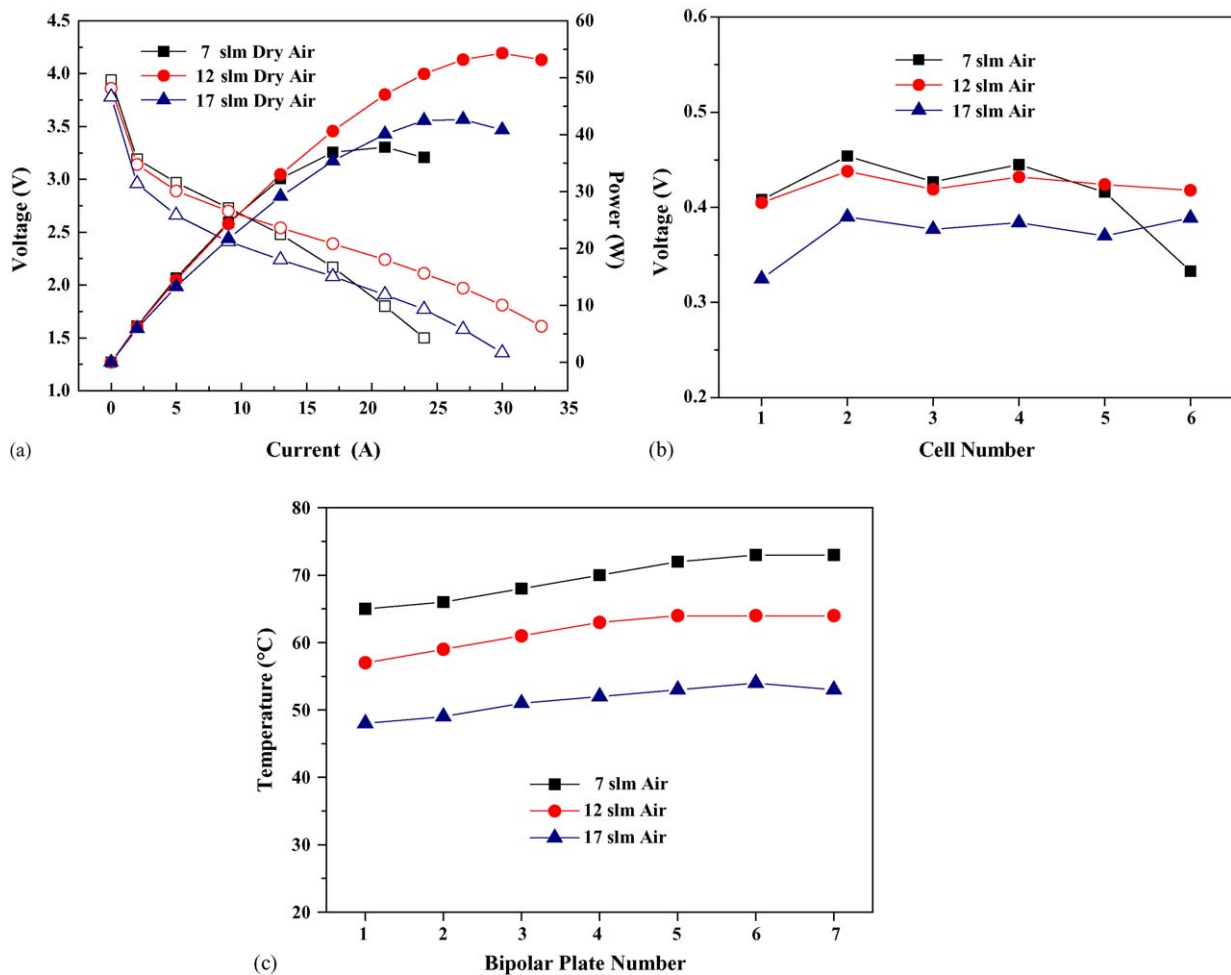

(a)

(b)

(c)

Fig. 7. (a) Stack power, (b) individual cell voltage, and (c) individual graphite plate temperature at different flow rates of dry air (■: 7 slm, ●: 12 slm, ▲: 17 slm dry air, 25 cm^3 min^{-1} 2 M methanol).

concentration of 1 M, the voltage distribution is non-uniform and the sixth cell has the lowest value. In contrast, with a methanol of 1.5 M and 2 M, the voltage difference between each cell diminishes, indicating that the voltage fluctuation over the unit cells might be due to non-uniform supply of methanol feed.

Fig. 6 shows the effect of the methanol flow rate on the stack performance in terms of the average voltage and power. The maximum performance is observed at flow rates between 25 ml min^{-1} and 35 ml min^{-1}. Fig. 6(b) shows the voltage distribution of individual cells in a stack at a constant current of 13 A (122 mA cm^{-2}). At a methanol flow rate of 15 ml min^{-1} (2.5 ml min^{-1} per cell), appreciable discrepancies exist among the cells; at higher flow rates, however, the voltage distribution is more uniform. As mentioned, the non-uniform voltage distribution might be due to the non-uniform activity of the MEAs in the stack and the uneven distribution of the feed (air and methanol) to the cells. In view of Fig. 6(b), we deduce that the uneven voltage distribution is caused by the non-uniform supply of methanol to the cells, and that the

unevenness could be mitigated by increasing the fuel flow rate.

Fig. 6(c) shows the outlet temperature of the methanol stream. At currents lower than 10 A, the largest methanol feed rate gives the lowest temperature. However, the order is reversed at currents higher than 10 A, and the temperature increase as the methanol flow rate increases. The dependence of the temperature on the methanol flow rate and on the electric load might be caused by the combined effect of the methanol crossover and the cooling by the methanol solution. At low currents, the heat generated at the cathode by the electrochemical reaction is insufficient; in addition, the methanol solution can act as a heat sink, causing the temperature to fall as the flow rate increases [16]. At high currents, on the other hand, the higher methanol flow rate induces higher methanol crossover to increase the temperature.

The flow rate of dry air has also influenced the performance of the stack as illustrated in Fig. 7. The maximum performance, which resulted from a compromise between the temperature and oxygen supply to the stack, occurred at 12 slm of dry air with a 2 M methanol solution
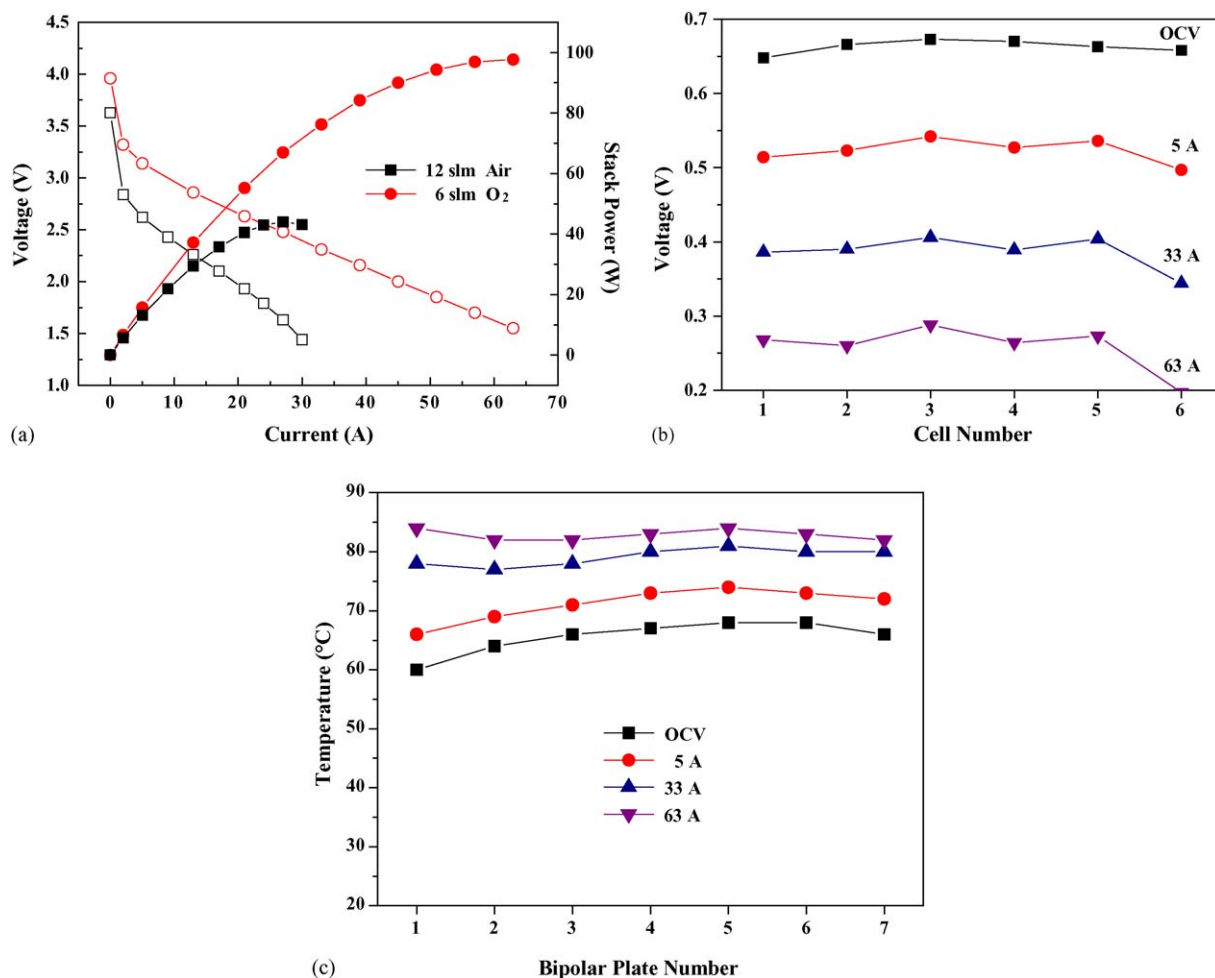

Fig. 8. (a) Stack power (■: 12 slm dry air, ●: 6 slm O$_2$), (b) individual cell voltage, and (c) individual graphite plate temperature at the oxygen supply (25 cm^3 min^{-1} 2 M methanol).

of 25 ml min^{-1}. Fig. 7(b) shows the voltage profile of the stack at a load of 13 A. At a low air flow rate of 7 slm, the profile is non-uniform and the sixth cell has the lowest voltage. However, the profile flattens as the air flow rate increases, and the temperature of each cell depends on the air flow rate. In addition, as shown in Fig. 7(c), the temperature decreases as the flow rate increases, indicating that the heat dissipated by air is more pronounced than the heat produced by the oxygen reduction at the cathode and the oxidation of the crossover methanol, though the heat contribution by the methanol crossover increases due to pervaporation function of the membrane as the air flow rate increases [14]. An appropriate air flow rate is therefore needed to supply sufficient oxygen to the stack while minimizing the temperature drop.

To understand the influence of partial pressure of oxygen on the stack performance, we applied pure oxygen to the cathode and compared the results with the results of dry air. As shown in Fig. 8(a), the maximum power of the stack for 6 slm of pure oxygen was 95 W at 1.8 V, which is about twice the air under the given conditions. This experiment was conducted a month after the first set of experiments and, thus, the performance deteriorated by 18%. A similar decay of the stack performance was reported by Buttin et al. [13]. However, as can be seen from the voltage profile in Fig. 8(b), there was no

abrupt deterioration of certain cells, indicating that the performance of all cells had declined to the same degree. This decay is presumably due to the general degradation processes in DMFCs, such as the surface oxidation of the cathode catalyst, the loss of the electrochemically active surface area of the electrodes, the ruthenium crossing from the anode to the cathode, and the loss of the hydrophobic properties of the cathode [17].

Fig. 8(c) shows the temperature distribution in the stack, and one can see that the distribution follows almost the same trend as in the air stack in Fig. 7(c). However, in BP 1, which was located next to the methanol inlet, the temperature started to increase from 33 A and it climbed higher than the other unit cells at a high current of 63 A, probably because the heat produced at the cathode was sufficient to overcome the heat dissipation by the incoming methanol stream. The average stack temperature increased as the current increased, and eventually reached 84 °C at a current of 63 A. To extract a current higher than about 63 A, one may therefore need to employ cooling system that can keep the stack temperature below 80 °C or so.

The flow direction of the reactants must be determined to enable a uniform distribution of the reactants and temperature over all the cells and to facilitate removal of the reaction products, water and CO_2. In general, the counter-flow system is preferred because it is considered more advantageous to the distribution of reactants and temperature. As shown in Fig. 1(c), we compared two types of flow systems, namely the co-flow and counter-flow. Fig. 9 shows the results. The counter-flow system performs better than the co-flow system by more than 20%. The lower performance of the co-flow system may be attributed to two factors. First, because of the simultaneous variation in the concentrations of the two reactants oxygen and methanol, the rates of the electrochemical reactions decrease along the flow path, resulting in inefficient use of the MEA. Second, because the air is supplied from the bottom inlet of the stack in this co-flow system, the water
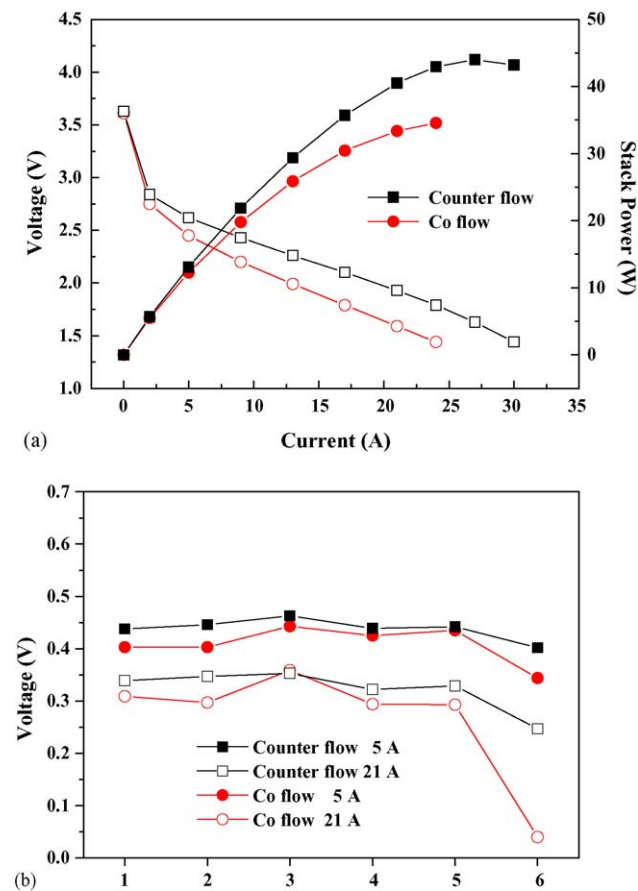

(a)

(b)

Fig. 9. (a) Stack power and (b) individual cell voltage at the counter-flow (■) and co-flow (●) system (25 cm^3 min^{-1} 2 M methanol, 12 slm dry air).
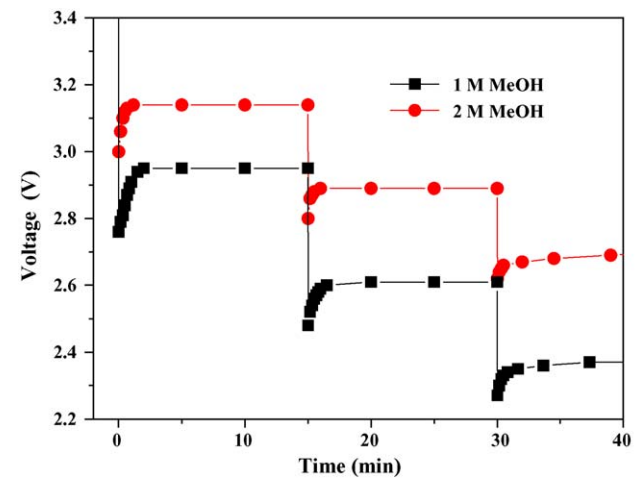

Fig. 10. Transient behavior of the stack at 1 M (■) and 2 M (●) methanol (25 cm^3 min^{-1} methanol solution, 12 slm dry air).

produced in the cathode may not be easily removed but accumulate in the cathode compartment to cause local flooding. As shown in Fig. 9(b), which compares the voltage distribution of the two systems, the counter-flow system has a more uniform distribution than the co-flow system.

The transient behavior of the stack that appears during the load change is another issue in fuel cells. As shown in Fig. 10, when an electric load of 2 A was applied to the stack, the voltage experienced an abrupt drop from the open circuit voltage (OCV) of 3.77–3.00 V for the 2 M methanol feed and then quickly recovered to reach a stabilized value of 3.14 V in 70 s. When the load was increased, the degree of fluctuation appeared somewhat reduced. In the case of the 1 M methanol feed, the voltage dropped from 3.84 V to 2.76 V at a load of 2 A and it climbed to a steady-state value of 2.95 V in 120 s. That is, the lower methanol feed concentration has the larger voltage drop and longer recovery time. This type of load following characteristic can be attributed to the mass transfer characteristics of the cells and the time scales required for the diffusion of methanol to the catalyst layers; and, thus, the characteristics are also affected by the methanol flow rate, the air flow rate, and the pressure in the cathode [16,18]. Moreover, the initial sharp decline in the voltage when the load is applied is related to the methanol crossover [19].

After optimizing the concentration, the flow rate and the flow direction of the reactants in the stack, we operated an LCD TV monitor that consumed about 20 W. For the monitor, we used a homemade DMFC system, which consisted of a DMFC stack, a DC–DC converter, an air blower, a methanol pump, and a methanol reservoir. We then used a micro-pump to feed a 1.5 M methanol solution from the methanol reservoir into the stack, after which the non-reacted methanol was circulated. Dry air was supplied with the aid of an air pump, and the DC–DC converter transformed the output voltage from 3 V to 12 V with an efficiency of about 75%. The LCD monitor with the present DMFC stack could be operated for nearly 2.5 h and the continued operation was hindered, which

was probably due to the accumulation of water in the cathode and the shortage of methanol in the reservoir. We are now planning to make an advanced DMFC system with a smart stack and with balance-of-plants (BOPs) to operate a laptop computer (Fig. 11).

4. Conclusion

A six-cell DMFC stack was prepared and the characteristics of the stack were compared with the single-cell data. The maximum power density of the single cell, which has an active area of 106 cm^2, was 95 mW cm^{-2} at 7.5 cm^3 min^{-1} of 2 M methanol and 750 sccm dry air. Although the single cell was operated at room temperature, its internal temperature increased to as high as 53 °C under the given conditions due to the heat released by the chemical oxidation of the crossover methanol and the oxygen reduction at the cathode.

The performance of the stack was affected by operating conditions such as the methanol concentration, the reactant flow rate, and the direction of the reactants in the stack. In the stack, the temperature was autonomously increased higher than the single cells and it rose as the electric load increased and as the feed flow rates decreased. At a high current range, the stack temperature climbed higher than 80 °C. An appropriate cooling system may therefore be needed to suppress the run-away temperature mise. Alternatively, the operating conditions should be chosen to constrain the excessive heat release.

The performance distribution of the individual cells in the stack strongly depended on the operating conditions, especially on the supply of the reactants. The higher flow rates of the reactants, methanol and air, may ensure a uniform supply of the reactants over all the cells, but it could reduce the stack temperature by heat dissipation. The optimum operating condition is therefore a compromise between the uniform supply of the reactants and the temperature. The counter-flow system is better than the co-flow system. By optimizing the operating conditions, we could achieve a maximum power of 54 W with the six-cell stack under 25 ml min^{-1} of 2 M methanol and 12 slm of dry air, at room temperature and atmospheric pressure.

In the test run of the DMFC system, we used the 50 W class stack together with BOPs to power an LCD TV. As a result, we confirmed the DMFC system's potential as a portable power source, though many hurdles still need to be overcome before it can be commercialized.

Fig. 11. Photograph of an LCD TV monitor turned on by the six-cell DMFC stack with a DC–DC converter.

References

[1] K. Scott, P. Argyropoulos, K. Sundmacher, J. Electroanal. Chem. 477 (1999) 97–110.
[2] K. Scott, W.M. Taama, P. Argyropoulos, K. Sundmacher, J. Power Sources 83 (1999) 204–216.
[3] J.-H. Kim, H.Y. Ha, I.-H. Oh, S.-A. Hong, H.-I. Lee, J. Power Sources 135 (2004) 29–35.

[4] A. Blum, T. Duvdevani, M. Philosoph, N. Rudoy, E. Peled, J. Power Sources 117 (2003) 22–25.

[5] R. Dillon, S. Srinivasan, A.S. Aricò, V. Antonucci, J. Power Sources 127 (2004) 112–126.

[6] B.-K. Kyo, I.-H. Oh, S.-A. Hong, H.Y. Ha, Electrochim. Acta 50 (2004) 781–785.

[7] D. Kim, E.A. Cho, S.-A. Hong, I.-H. Oh, H.Y. Ha, J. Power Sources 130 (2004) 172–177.

[8] A. Heinzel, C. Hebling, M. Müller, M. Zedda, C. Müller, J. Power Sources 105 (2002) 250–255.

[9] R. Jiang, D. Chu, J. Power Sources 93 (2001) 25–31.

[10] A. Kumar, R.G. Reddy, J. Power Sources 129 (2004) 62–67.

[11] R. Jiang, C. Rong, D. Chu, J. Power Sources 126 (2004) 119–124.

[12] H. Dohle, H. Schmitz, T. Bewer, J. Mergel, D. Stolten, J Power Sources 106 (2002) 313–322.

[13] D. Buttin, M. Dupont, M. Straumann, R. Gille, J-C. Dubois, R. Ornelas, G.P. Fleba, E. Ramunni, V. Antonucci, A.S. Aricò, P. Cretì, E. Modica, M. Pham-Thi, J-P. Ganne, J. Appl. Electrochem. 31 (2001) 275–279.

[14] V. Gogel, T. Frey, Z. Yongsheng, K.A. Friedrich, L. Jörissen, J. Garche, J. Power Sources 127 (2004) 172–180.

[15] M.K. Ravikumar, A.K. Shukla, J. Electrochem. Soc. 143 (1996) 2601–2606.

[16] P. Argyropoulos, K. Scott, W.M. Taama, Electrochim. Acta 45 (2000) 1983–1998.

[17] P. Piela, P. Zelenay, Performance durability issues in DMFC operation, in: 205th Meeting of the Electrochemical Society, Texas, USA, 9–14 May, 2004, Abs 338.

[18] P. Argyropoulos, K. Scott, W.M. Taama, J. Appl. Electrochem. 31 (2001) 13–24.

[19] Z. Qi, A. Kaufman, J. Power Sources 110 (2002) 177–185.